Elastic and inelastic scattering of ^{8}Li from ^{12}C

R. J. Smith, J. J. Kolata, K. Lamkin, and A. Morsad*
Physics Department, University of Notre Dame, Notre Dame, Indiana 46556

F. D. Becchetti, J. A. Brown, W. Z. Liu,† J. W. Jänecke, and D. A. Roberts
Physics Department, University of Michigan, Ann Arbor, Michigan 48109

R. E. Warner
Physics Department, Oberlin College, Oberlin, Ohio 44074
(Received 28 December 1990)

Elastic and inelastic scattering of ^{8}Li ions have been observed on targets of C and Au at a beam energy of 14 MeV, using the University of Notre Dame–University of Michigan radioactive nuclear beam facility. The elastic scattering shows that, in most respects, ^{8}Li behaves similarly to ^{6,7}Li. However, a large probability for populating the first excited state of ^{8}Li via inelastic scattering is observed. Data analysis using a deformed optical-model potential obtained from fits to the elastic scattering yields a reduced transition strength $B(E2\uparrow)=30\pm15\ e^2\,\mathrm{fm}^4$.

I. INTRODUCTION

The unusual reaction Q values, spins, and isospins of neutron-rich and proton-rich short-lived radioactive nuclei motivate their use as secondary radioactive nuclear beams (RNB) in a variety of reaction studies, e.g., elastic and inelastic scattering, and transfer reactions. The University of Notre Dame–University of Michigan RNB facility[1–3] has been used to survey a number of such reactions at low bombarding energies, principally using a 14-MeV ^{8}Li beam; the first set of results, involving the (^{8}Li,^{7}Li) reaction, has recently been published.[3] We report here a measurement and optical-model analysis of the elastic and inelastic scattering of ^{8}Li on a C target. Preliminary reports of this work have appeared elsewhere.[4]

II. EXPERIMENTAL METHOD

Secondary beams of 13.8–14.9-MeV ^{8}Li ions, having an energy spread of 400–600 keV full width at half maximum (FWHM), are produced via the ^{9}Be (^{7}Li,^{8}Li) ^{8}Be$_{g.s.}$ reaction using a 17-MeV ^{7}Li primary beam incident on a 12.7-μm-thick ^{9}Be production target. The ^{8}Li reaction products in the angular range from 5° to 11° in the laboratory system are collected and refocused into a 5-mm-diam beam spot using a 3.5-T superconducting solenoid lens; the resulting beam has an angular divergence of $\pm3°$. The direct and scattered ^{7}Li ions are removed by a series of beam blocks, so that the beam is of high purity.[1,2]

Recent improvements to the facility have included the installation of a high-intensity negative-ion sputter source that produces up to 10 particle microamperes ($p\,\mu$A) of ^{7}Li, and the replacement of the stationary Be production target with a large-area target that can be rotated at angular speeds up to 100 rpm. At present, the ^{7}Li current on target is limited to about 2 $p\,\mu$A due to beam-heating and related effects. Nonetheless, the maximum secondary-beam intensity is approximately 1×10^{7} sec^{-1}. Another improvement was to make the scattered-beam block movable along the solenoid axis (z axis). The movable z-axis block, together with suitable small adjustments in the solenoid focusing current and the use of additional "beam-scraper" apertures, enables us to minimize low-energy tails and spurious lower-energy peaks[4] in the secondary beam at some expense in intensity.

The reaction products were detected and identified using a ΔE-E, XY position-sensitive counter telescope. The ΔE detector was typically a 10–23-μm-thick, 100–300-mm^2 Si surface-barrier (SSB) detector and was backed by a 25 mm$\times$25 mm, 200-μm-thick XY position-sensitive SSB detector. The primary- and secondary-beam intensities were monitored by additional SSB detectors located in both the production and secondary target chambers. The energy profile and intensity of the ^{8}Li beam was measured directly by placing the detector telescope in a direct beam of much-reduced intensity, and also by Rutherford scattering from a Au foil of known thickness (Figs. 1 and 2). These two methods typically agreed to within $\pm15\%$, which is comparable to the uncertainties in the thicknesses of the targets used for these normalizations.

Targets of 0.6–3-mg/cm^2 $^{\mathrm{nat}}$CH$_2$, $^{\mathrm{nat}}$CD$_2$, $^{\mathrm{nat}}$C, and Au were used in this experiment. Elastic and inelastic ^{8}Li+C spectra taken with different ΔE detectors are shown in Figs. 3 and 4. The thinnest ΔE detector (10 μm) permitted measurements up to $E_x=6$ MeV in ^{8}Li or C, while the 17–28-μm ΔE detectors provided better particle identification but over a more limited range in excitation energy. For this reason, only a few measurements of inelastic scattering to the first excited state of ^{12}C were obtained. Note that the energy spectra in Figs. 3 and 4 have been corrected for kinematic shifts ($dE/d\theta$) using the XY information from the detector telescope. This correction was especially necessary for the larger-area ΔE detectors. The position information was also used to sub-

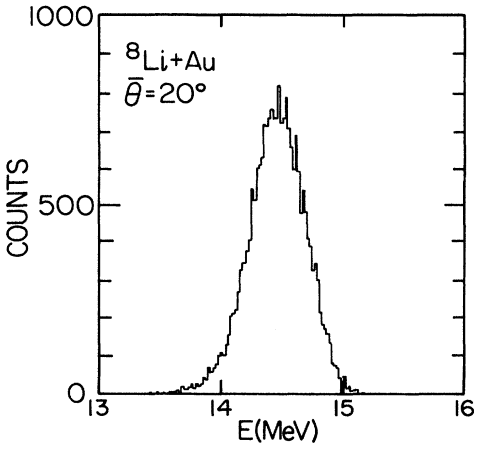

FIG. 1. Energy profile of the ^{8}Li beam as determined by elastic scattering from a 0.86-mg/cm^2 Au target. (Note the zero offset on the energy scale.)

divide these large detectors into angular regions, typically a few degrees wide, for the determination of angular distributions.

In addition to the elastic scattering, the excitation of the (1^+, E_x=0.98 MeV) first excited state of ^{8}Li was also observed (Figs. 3 and 4). This group appears as a distinct shoulder, at the correct excitation energy, on the spectra from ^{8}Li+C, and was also seen in similar spectra taken with targets of ^{9}Be and ^{13}C. The group tracks in angle with the kinematics expected for ^{8}Li scattered from ^{12}C, and thus does not appear to originate in elastic scattering from light target contaminants. One possible explanation is the contamination of the beam with ^{8}Li ions produced via the ^{9}Be(^{7}Li,^{8}Li$^*_{0.98}$)^{8}Be$_{g.s.}$ reaction at the production target which has, in fact, been observed.[4] However, as noted above, most of this source of contamination was removed with the installation of the movable beam block, and we therefore assign the group seen at about E_x=1 MeV to the projectile excitation of ^{8}Li by the secondary target. In addition, in earlier runs where such contamination was observed, it could be monitored (and subtracted out) by observing the scattering of the ^{8}Li beam from Au.

Another possible problem is contamination of the ^{8}Li spectra by ^{7}Li ions coming from the ^{12}C(^{8}Li,^{7}Li)^{13}C reaction. The transfer to the ($\frac{5}{2}^+$, E_x=3.85 MeV) state in ^{13}C has a very large cross section[3] (30–100 mb/sr) at forward angles, and the Q value is such that it can interfere with measurements of the ^{8}Li$_{g.s.}$, as well as ^{8}Li$^*_{0.98}$. This is particularly true for measurements[4] employing the thinnest ΔE detectors, which have poor isotope separation. Therefore, a set of measurements was made with a highly planar 22-μm ΔE detector which gave a clean separation of ^{8}Li from ^{7}Li, and hence adequate determination of the ^{8}Li$^*_{0.98}$ cross section.

The ^{8}Li elastic- and inelastic-scattering angular distributions are shown in Figs. 5–7. These incorporate data

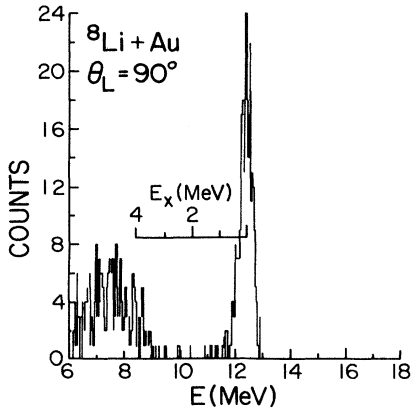

FIG. 2. A large-angle ^{8}Li+Au scattering spectrum taken at a beam energy of 14 MeV.

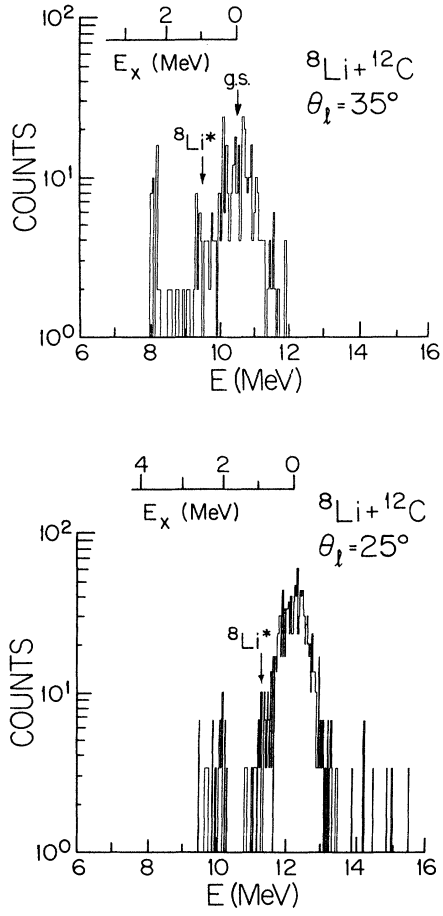

FIG. 3. Energy spectra from the C(^{8}Li,^{8}Li) reaction at a laboratory energy of 14 MeV. The target was 0.59 mg/cm^2 of natural C. The upper spectrum was taken with a thin (10-μm) ΔE detector, while the lower spectrum was taken with a 17-μm ΔE detector.

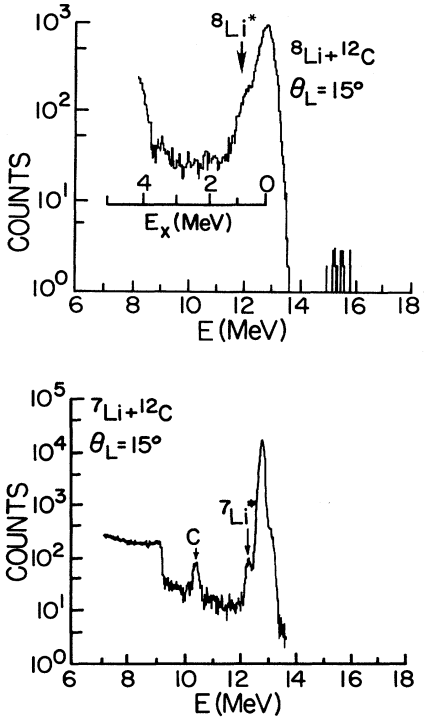

FIG. 4. A comparison of spectra taken for ^{7,8}Li+C at $E_{lab}=14$ MeV and $\theta_{lab}=15°$. The group labeled "*C*" in the lower panel is a ^{6}Li contaminant from the (^{7}Li,^{6}Li) reaction.

taken during several running periods, using different targets and ΔE detectors of various thicknesses and areas. The mean scattering angles are calculated from the *XY* position information and the angle setting of the detector

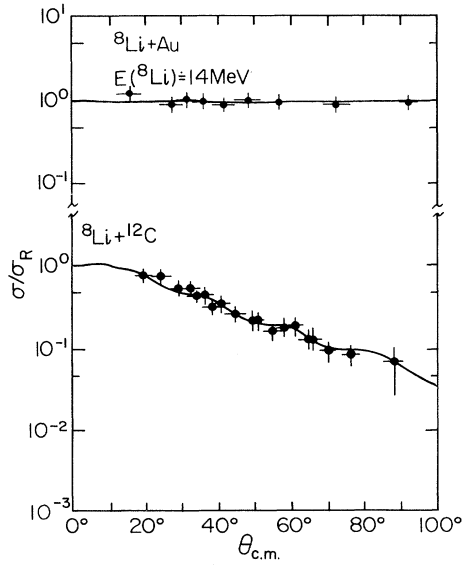

FIG. 5. Elastic-scattering angular distributions for ^{8}Li from C and Au targets compared with optical-model calculations using the adopted best-fit parameters (set *F*, Table I).

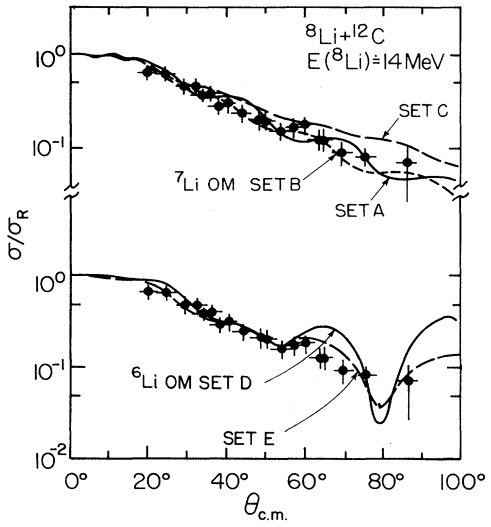

FIG. 6. Comparison of ^{8}Li+C elastic-scattering data with OM predictions using published ^{7}Li+^{12}C and ^{6}Li+^{12}C parameter sets (Table I).

telescope. They are estimated to be accurate to ±2°. The normalization of the forward-angle elastic-scattering data is more uncertain due to the effective ±4° spread in angle resulting from the beam divergence and the finite beam spot size, combined with the rapid falloff of the Rutherford cross section. The large-angle data are less affected

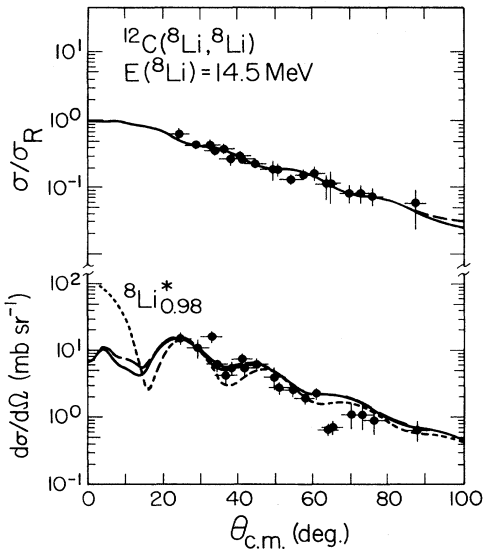

FIG. 7. Elastic- and inelastic-scattering angular distributions for ^{8}Li+C, compared with PTOLEMY calculations (see text). The solid and dashed curves are $L=2$ calculations with $B(E2\uparrow)=30$ and 45 e^2fm^4, respectively, to illustrate the lack of sensitivity to Coulex in the region where data are available. The dotted curve is an $L=0$ prediction arbitrarily normalized to the experimental data.

by these problems and were therefore used whenever possible for the absolute normalization to the ^{8}Li+Au scattering. The latter falls off as expected for pure Rutherford scattering (Fig. 5), as one might anticipate for a bombarding energy that is 6 MeV below the calculated Coulomb barrier. On the other hand, it is possible that neutron-rich RNB such as ^{8}Li might not scatter according to the Rutherford formula even at energies well below the classical Coulomb barrier due to strong couplings to inelastic or transfer channels, especially since many of the transfer channels have positive Q values. Therefore, the angular distribution for ^{8}Li+Au in Fig. 5 is a nontrivial result.

In addition to measurements using the secondary ^{8}Li beam, experiments were performed with a direct ^{7}Li beam on the same C and Au targets (Fig. 4) to verify the purity and thicknesses of the targets and to provide comparison data on ^{7}Li+C elastic and inelastic scattering, although, in practice, the comparison was primarily made with data taken from the literature as discussed below. In this case, contamination from the (^{7}Li,^{6}Li) reaction appears at large negative excitation energy, due to the negative-Q value for this reaction.

III. ANALYSIS

As noted above, some ^{6,7}Li elastic-scattering data for ^{12}C targets at beam energies of approximately 14 MeV are available from the present experiment and also from earlier work,[5] while many analyses[6–11] exist for energies greater than 20 MeV. In Fig. 6, we compare our ^{8}Li+C elastic data with optical-model (OM) calculations using published ^{6}Li and ^{7}Li OM potentials.[5–8] The elastic-scattering data at large angles show that the absorption cross sections for ^{8}Li and ^{7}Li are quite similar, and greater than that observed for ^{6}Li.

These and other published ^{6,7}Li OM parameter sets[5–11] were investigated as starting points for a more complete analysis of our data. In general, the ^{6}Li parameter sets resulted in more highly diffractive elastic angular distributions than observed, and also provided somewhat poorer fits to the inelastic data than parameter sets based on ^{7}Li scattering. We therefore used the ^{7}Li+^{12}C parameter set from Ref. 7 as our starting point. Minor changes in the real potential depth and radius, together with more extensive adjustments in the imaginary potential, produced the fit illustrated in Fig. 5. The corresponding best-fit OM parameters appear as set F in Table I. It should be noted that the ^{8}Li ground state has $J^{\pi}=2^{+}$, so that the spin-orbit interaction, which has been neglected in most Li OM analyses, including the present one, may be contributing to the observed differences in ^{6,7,8}Li elastic scattering. Another possibly important effect that has been neglected is coupling to the ^{8}Li* inelastic-scattering channel, which has been found to be important for ^{7}Li. Coupling to the first excited state can account[7,8] for the reduction in the diffractive behavior of large-angle elastic scattering of ^{7}Li relative to ^{6}Li.

Our adopted best-fit OM potential set is not unique, and other families of potentials can be found which give similar fits to the elastic- and inelastic-scattering data. The volume integrals of this potential are, however, compatible with the potential family one expects on the basis of most low-energy ^{6,7}Li scattering studies,[5–9] but substantially less than those predicted using the "unique" parameter set determined[11] by Nadasen *et al.* for ^{6}Li scattering at energies greater than 100 MeV. The calculated ^{8}Li total reaction cross section at 14 MeV using our best-fit potential is 1367 mb, similar to that for ^{6,7}Li. In terms of the interaction radius, therefore, ^{8}Li is "normal," as opposed to the large interaction radii deduced[12,13] for ^{9,11}Li (at much higher energies). The latter results are, however, inferred from beam-attenuation and γ-ray measurements and may not be very precisely related to interaction radii determined from OM total reaction cross sections. As more intense beams of ^{9,11}Li become available, it should be possible to deduce the interaction radii from elastic-scattering studies as in the present experiment.

The angular distribution deduced for excitation of the ^{8}Li$^{*}_{0.98}$ state, and the data obtained at a few selected angles for ^{12}C$^{*}_{4.44}$, were analyzed using our best-fit ^{8}Li+^{12}C OM parameter set (Table I), and collective-model form factors.[14] The extraction of the relevant deformation pa-

TABLE I. ^{8}Li+^{12}C optical-model parameters.

OM set	Source	V_R[a] (MeV)	R_R (fm)	a_R (fm)	W[a] (MeV)	R_w (fm)	a_w (fm)	R_c (fm)	Ref.
A	^{7}Li+^{12}C $E(^{7}\text{Li})=13$ MeV	−166	3.37	0.65	−26[b]	3.37[b]	0.65[b]	5.57	6
B	^{7}Li+^{12}C $E(^{7}\text{Li})=36$ MeV	−188	2.76	0.82	−13	4.97	0.77	2.97	7
C	^{7}Li+^{12}C $E(^{7}\text{Li})=4.5$–88 MeV	−167	2.57	0.80	−9.6	5.61	0.72	5.36	8
D	^{6}Li+^{12}C $E(^{6}\text{Li})=13$ MeV	−148	3.37	0.65	−8.5[b]	3.37[b]	0.65[b]	5.57	6
E	^{6}Li+^{12}C $E(^{6}\text{Li})=4.5$–156 MeV	−154	2.61	0.79	−4.4	5.75	0.62	5.36	8
F	^{8}Li+^{12}C $E(^{8}\text{Li})=14$ MeV	−172	2.97	0.80	−15	5.15	0.80	5.36	This work

[a]Volume Woods-Saxon potential unless otherwise noted.
[b]Surface-derivative Woods-Saxon potential.

rameters from such an analysis is fraught with ambiguities,[14] especially when the empirical optical-model potential has very different geometries in its real and imaginary parts as in the present case. For example, one might choose to equate the deformation parameters β_L of the real and imaginary parts of the potential, but another possibility is to equate the deformation lengths, i.e.,

$$\beta_{\text{real}} R_R = \beta_{\text{imag}} R_W \ . \tag{1}$$

In addition, the transition we are studying is probably dominated by $L=2$, but with a possible $L=0$, $S=1$ admixture from spin-flip excitation that is not well modeled in the present case because of the neglect of the spin-orbit term in our optical-model potential. Because of these and other ambiguities, we decided to extract the deformation parameters from a comparison with existing ^{7}Li+^{12}C data. The calculations were performed using the coupled-channels code PTOLEMY.[15] In the first instance, ^{7}Li (0.478 MeV) inelastic data[8] taken at $E_{\text{lab}}=34$ MeV were fitted using the accepted value[16] of $B(E2\uparrow)=8.3$ e^2fm^4, a deformation parameter $\beta_2=0.43$ for the real and imaginary parts of the deformed optical-model potential, and a deformation length for the projectile-excitation coupling $\delta_p=0.97$ fm which matches that of the imaginary potential. (The transition is presumed to be dominated by the imaginary potential due to its large radius.) The optical-model potential parameters were those deduced from our best-fit ^{8}Li analysis (set F, Table I), which differ only slightly from those used in a previous analysis[7] of the ^{7}Li data, and the fits obtained to the elastic and inelastic data (Fig. 8) are at least as good as those presented in this earlier work. In the next step, the calculation was repeated to fit our ^{8}Li data, and we determined the corresponding deformation parameters $\beta_2=0.72$ and $\delta_p=1.75$ fm. An electromagnetic transition strength $B(E2\uparrow)=30$ e^2fm^4 was chosen according to the method discussed below, but, in any case, the theoretical angular distribution is rather insensitive to the value of $B(E2\uparrow)$ over the range of the experimental data. The results of this calculation are shown by the solid curves in Fig. 7. It can be seen that the elastic-scattering cross section now tends to be very slightly underpredicted, since we have included explicit coupling to the first excited state without making a corresponding adjustment in the depth of the imaginary potential. This situation can be improved by an iteration of the fitting process, but it was not deemed necessary to do so in this case because of the remaining ambiguities which introduce comparable errors into the analysis. The inelastic data are also fitted reasonably well by this pure $L=2$ calculation, though the possible contribution of $L=0$ will be discussed further below. Although other models (and other choices for the deformation parameters) can give equivalent fits to the ^{7,8}Li data, we have found that the *ratio* of the ^{8}Li to ^{7}Li deformation lengths tends to remain approximately constant.

The transition strengths $B(E\lambda\uparrow)$ for the $i\rightarrow j$ transition are generally deduced[14] from the relation

$$\sigma^{\text{expt}}(\theta)=\beta_{ij}^2\sigma_L(\theta) \ , \tag{2}$$

where $\sigma_L(\theta)$ is the calculated cross section with deformation parameter β_L and for angular momentum transfer $\lambda=L$. In the rotational model, one has

$$\beta_{ij}^2=\langle J_i L K 0|J_f K\rangle^2\beta_L^2 \ , \tag{3}$$

where K is the projection of J_i onto the nuclear symmetry axis. The deformation parameter β_L is clearly model dependent, but $B(E2\uparrow)$ can, in principle, be extracted from β_{ij}^2 in a model-independent fashion. Unfortunately, different analyses have led to different values for β_{ij}^2 in the ^{7}Li case[6,8] due to the ambiguities described above, and we have found it necessary to normalize our results accordingly. The values for δ_p extracted from the ^{7,8}Li data imply a larger deformation for ^{8}Li, which is perhaps surprising considering that the measured static ground-state quadrupole moments[16] imply just the opposite; however, we are measuring the transition moment. The $B(E2\uparrow)$ for ^{8}Li was calculated by multiplying the corresponding value for ^{7}Li, determined from Coulex measurements, by the square of the ratio of the δ_p values. This results in a $B(E2\uparrow)$ $(2^+\rightarrow 1^+)=30\pm 15$ e^2fm^4, which is about four times larger than that deduced[16] for the $\frac{3}{2}^-\rightarrow\frac{1}{2}^-$ transition from the ground state to the first excited state of ^{7}Li. The experimental error is dominated by the uncertainty in the normalization procedure, due to the differences in the OM potential geometries that can be used to fit the inelastic-scattering data. It is appropriate to consider whether this large transition strength is consistent with a relatively pure $M1$ character[16] for the γ-ray decay of ^{8}Li$^*_{0.98}$. The corresponding mean life for $E2$ decay is 18 psec, while the measured lifetime[16] of the state is 12 ± 4 fsec, implying a small mixing ratio $\delta(E2/M1)=2.6\times 10^{-2}$. Next we compare with quadrupole transition strengths for other $T=1$ p-shell nuclei (Table II). In terms of the parameter β_2, deduced[17] from $B(E2\uparrow)$, ^{8}Li is apparently more deformed than ^{10}Be,

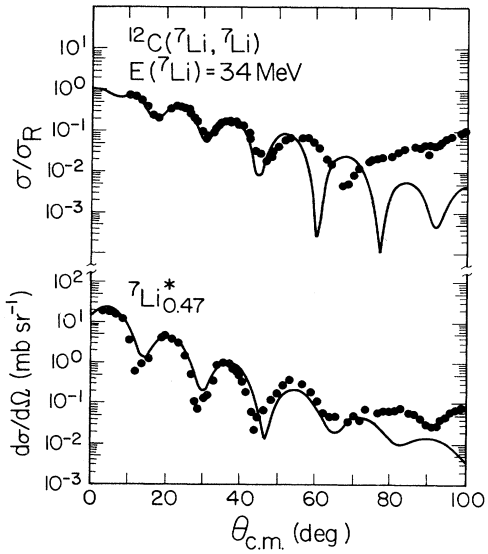

FIG. 8. Comparison of ^{7}Li+^{12}C data with PTOLEMY calculations (see text).

TABLE II. Comparison of transition strengths and quadrupole moments for $T=1$ p-shell nuclei.

Nucleus	$B(E2\uparrow)$ (e^2fm^4)	β_2	β_2/β_2^{SP}	Q_0 (b)	EWSR(I)[a] (%)	EWSR(II)[a] (%)
^{8}Li	30±15	1.3±0.3	2.5±0.6	0.31±0.07[b]	1.3±0.7	9.2±4.6
^{10}Be	52±6	1.13±0.06	2.84±0.16	0.229±0.013	5.3±0.6	33.1±3.8
^{10}C	62±10	0.82±0.07	3.11±0.25	0.250±0.020	6.3±1.0	17.5±2.8

[a]Energy-weighted sum rules. See Ref. 17.
[b]Assuming $K=1$.

which previously had the largest known value of β_2 (although the uncertainty in the value of β_2 is quite large for ^{8}Li). A somewhat different picture emerges when one normalizes to the single-particle value, which is proportional to Z^{-1}. In this comparison, ^{10}C has the largest deformation and ^{8}Li ranks third behind ^{8}Be. The transition quadrupole moments Q_0 are comparable for all three nuclei, and the percentages of the appropriate energy-weighted sum rules[17] indicate that, despite the large $E2$ strength in low-lying states in these nuclei, only a small fraction of the available strength has been exhausted.

Although a pure $L=2$ calculation (Fig. 7) provides an adequate fit to the experimental data, the possibility of an $L=0$ spin-flip ($\Delta S=1$) excitation must be considered, particularly since the ground-state spin of ^{8}Li ($J^\pi=2^+$) might result in a large spin-orbit coupling, and the $1^+\rightarrow 2^+$ γ-ray transition is dominated by $M1$. Such a calculation is also illustrated in Fig. 7. It can be seen that the predicted angular distribution is quite similar to that for $L=2$, and can only be distinguished at forward angles where we presently cannot take data due to the relatively large ($\pm 3°$) angular divergence of the ^{8}Li beam. This issue could be resolved in an experiment involving pure Coulomb excitation of the projectile, to which the $L=0$ mode contributes only weakly. Furthermore, Coulex experiments are not subject to the considerable ambiguities in the calculation of the inelastic form factor that plague the present work.

Finally, analysis of the limited amount of data obtained for excitation of the ^{12}C first excited state yields an upper limit $B(E2\uparrow)\leq 100$ e^2fm^4, which is consistent with the accepted value[17] of 41 ± 5 e^2fm^4. In addition, the absence of measurable inelastic-scattering cross section in the excitation energy region from 1.5 to 2.0 MeV allows us to set an upper limit $B(E1\uparrow)\leq 0.4$ e^2fm^2/MeV, which can be compared with the value of 0.1 e^2fm^2 deduced by Bertsch and Foxwell[18] for ^{11}Li. Thus, there is no evidence in the present data for "soft" $E1$ strength in ^{8}Li below the neutron decay threshold at 2 MeV.

IV. CONCLUSIONS

The elastic scattering of ^{8}Li on C has been measured at a laboratory energy of 14 MeV. Optical-model analysis has shown that the ^{8}Li projectile is absorbed in a manner quite similar to that of ^{7}Li. In fact, our best-fit OM potential can account quite well for the ^{7}Li+^{12}C data taken at 34 MeV by the Florida State group.[7,8] In contrast, the inelastic excitations of the first excited states of the two projectiles differ considerably, with the ^{8}Li nucleus displaying a much larger inelastic excitation probability. If interpreted in the context of a collective excitation, this result implies that $B(E2\uparrow)$ for the transition to the first excited state of ^{8}Li is four times greater than that for the corresponding transition in ^{7}Li. In this respect, ^{8}Li resembles ^{10}Be, another $T=1$ p-shell nucleus with a large transition quadrupole moment. However, the possibility of $L=0$ contributions to the measured cross section, and ambiguities in calculating the nuclear form factor in the collective model, suggest that Coulex experiments are necessary to confirm this result. Such experiments are currently in progress.

ACKNOWLEDGMENTS

We would like to thank R. Kryger, J. Bajema, S. Dixit, R. Tighe, Dr. E. D. Berners, and Dr. X. J. Kong for their generous help during various stages of this experiment. We also thank Dr. G. R. Satchler, Dr. K. T. Hecht, and Dr. K. Kemper for assistance in interpreting the data. This work was supported by the U.S. National Science Foundation (NSF) under Contract Nos. PHY88-03035, PHY86-05907, PHY89-11831, and PHY89-00070.

*Present address: Centre de Recherches Nucleaires and Universite Louis Pasteur, 67037 Strasbourg CEDEX, France.
†Present address: Cyclotron Institute, Texas A&M University, College Station, TX 77843.

[1]J. J. Kolata, A. Morsad, X. J. Kong, R. E. Warner, F. D. Becchetti, W. Z. Liu, D. A. Roberts, and J. W. Jänecke, Nucl. Instrum. Methods Phys. Res. **B40-41**, 503 (1989).
[2]F. D. Becchetti, W. Z. Liu, D. A. Roberts, J. W. Jänecke, J. J. Kolata, A. Morsad, X. J. Kong, and R. E. Warner, in *Proceedings of the International Symposium on Heavy Ion Physics and Nuclear Astrophysical Problems, Tokyo, 1988* (World-Scientific, Singapore 1989), p. 277; W. Z. Liu, Ph. D. thesis, University of Michigan, 1990.
[3]F. D. Becchetti, W. Z. Liu, D. A. Roberts, J. W. Jänecke, J. J. Kolata, A. Morsad, X. J. Kong, and R. E. Warner, Phys. Rev. C **40**, R1104 (1989).

[4]W. Z. Liu *et al.*, in *Proceedings of the First International Conference on Radioactive Nuclear Beams,* edited by W. D. Myers, J. M. Nitschke, and E. B. Norman (World-Scientific, Singapore, 1990), p. 499; J. Brown *et al.*, *ibid.*, p. 372; F. D. Becchetti *et al.*, *ibid.*, p. 305.

[5]J. E. Poling, E. Norbeck, and R. R. Carlson, Phys. Rev. C **5**, 1819 (1972); K. A. Weber, K. Meier-Ewert, H. Schmidt-Böcking, and K. Bethge, Nucl. Phys. **A186**, 145 (1972).

[6]P. Schumacher, N. Ueta, H. H. Duhm, K.-I. Kubo, and W. J. Klages, Nucl. Phys. **A212**, 573 (1973).

[7]M. F. Vineyard, J. Cook, K. W. Kemper, and M. N. Stephens, Phys. Rev. C **30**, 916 (1984).

[8]M. F. Vineyard, J. Cook, and K. W. Kemper, Phys. Rev. C **31**, 879 (1985); J. Cook, Nucl. Phys. **A445**, 350 (1985); J. Cook, M. N. Stephens, K. W. Kemper, and A. K. Abdallah, Phys. Rev. C **33**, 915 (1986).

[9]L. T. Chua, F. D. Becchetti, J. Jänecke, and F. L. Milder, Nucl. Phys. **A273**, 243 (1976).

[10]P. Schwandt, W. W. Jacobs, M. D. Kaitchuck, P. P. Singh, W. D. Ploughe, F. D. Becchetti, and J. Jänecke, Phys. Rev. C **24**, 1522 (1981).

[11]A. Nadasen, M. McMaster, G. Gunderson, A. Judd, S. Villanueva, P. Schwandt, J. S. Winfield, J. van der Plicht, R. E. Warner, F. D. Becchetti, and J. W. Jänecke, Phys. Rev. C **37**, 132 (1988); A. Nadasen, M. McMaster, M. Fingal, J. Tavormina, J. S. Winfield, R. M. Ronningen, P. Schwandt, F. D. Becchetti, J. W. Jänecke, and R. E. Warner, *ibid.* **40**, 1237 (1989).

[12]I. Tanihata, H. Hamagaki, O. Hashimoto, Y. Shida, N. Yoshikawa, K. Sugimoto, O. Yamakawa, T. Kobayashi, and N. Takahashi, Phys. Rev. Lett. **55**, 2676 (1985).

[13]W. Mittig *et al.*, Phys. Rev. Lett. **59**, 1889 (1987).

[14]G. R. Satchler, Nucl. Phys. **A491**, 413 (1989); G. R. Satchler, *Direct Nuclear Reactions* (Oxford University, Oxford, 1983).

[15]D. H. Gloeckner, M. H. Macfarlane, and S. C. Pieper, Argonne National Laboratory Report No. ANL-76-11, 1976 (unpublished); M. Rhoades-Brown, M. H. Macfarlane, and S. C. Pieper, Phys. Rev. C **21**, 2417 (1980).

[16]F. Ajzenberg-Selove, Nucl. Phys. **A490**, 1 (1988).

[17]S. Raman, C. H. Malarkey, W. T. Milner, C. W. Nestor, and P. H. Stelson, At. Data Nucl. Data Tables **36**, 1 (1987).

[18]G. R. Bertsch and J. Foxwell, Phys. Rev. C **41**, 1300 (1990).